Electronic-structure calculations at macroscopic scales

M. Ortiz
California Institute of Technology

In collaboration with: **K. Bhattacharya** (Caltech), **T. Blesgen** (Leipzig), **V. Gavini** (UMich), **J. Knap** (ARL), **P. Suryanarayana** (Caltech)

8th World Congress on Computational Mechanics
Venezia, June 30, 2008

Introduction – Defective crystals

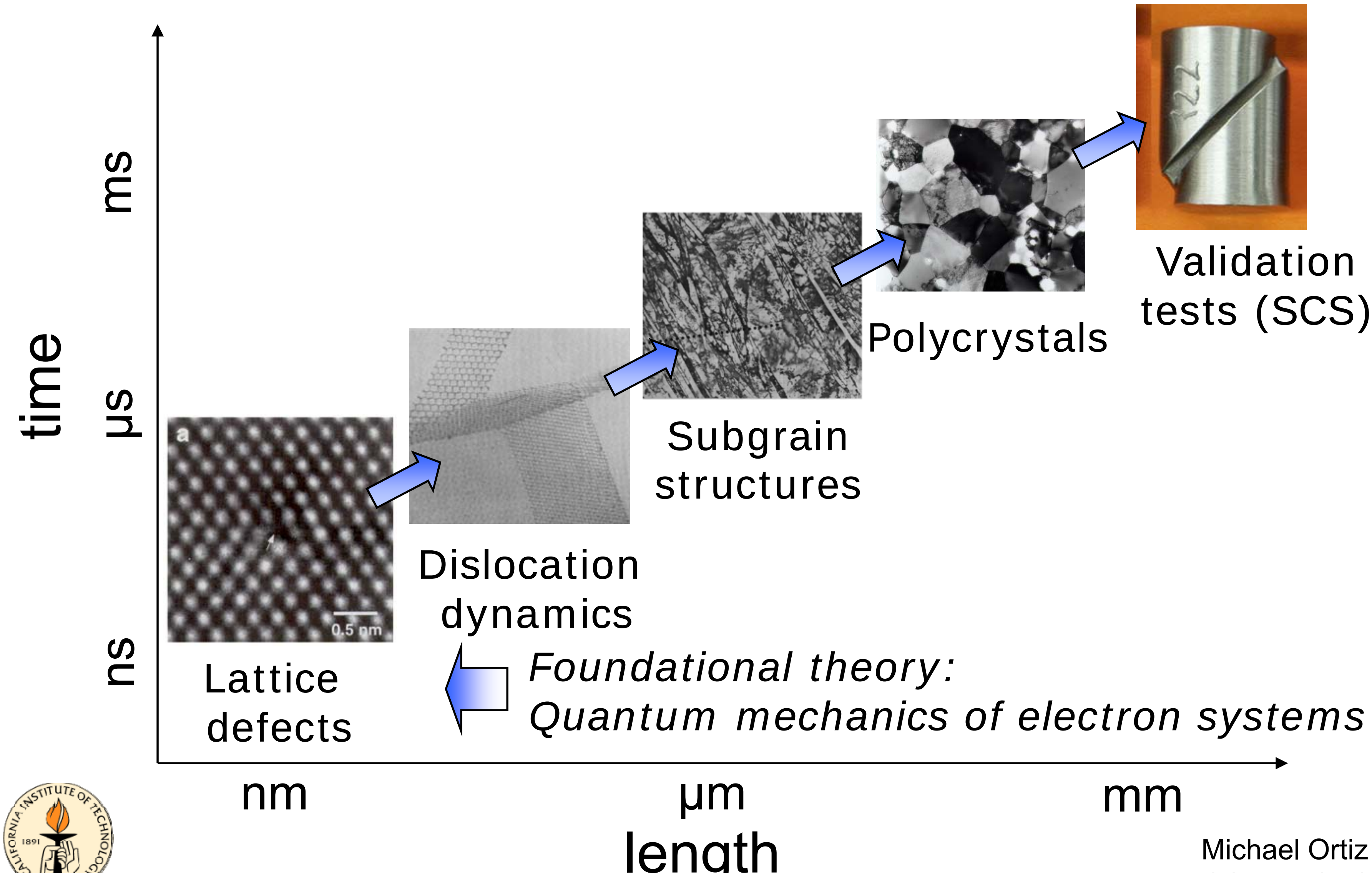

Introduction – Defective crystals

"Crystals are like people. It is the defects in them that make them interesting."

-- Sir F. Charles Frank

Introduction – Defective crystals

- The *accurate* calculation of many fundamental properties of crystal defects requires careful consideration of their *electronic structure*…
- Example: *Ab initio* screw dislocation cores in bcc metals. (a) Ta easy, (b) Ta hard; and (c) Mo easy (S. Ismail-Beigi and T.A. Arias, 1999)
- But: Finnis-Sinclair predicts ‘easy core’ structure only! (A. Ramasubramanian, M.P. Ariza and M. Ortiz, *JMPS*, 2007)

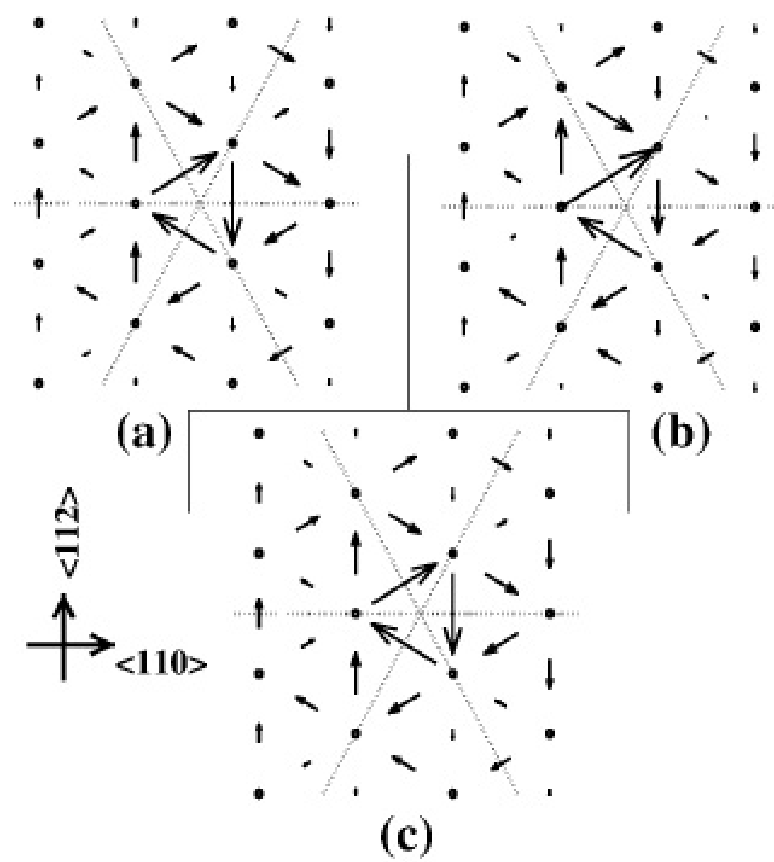

Introduction – Defective crystals

Empirical interatomic potentials do not afford sufficient accuracy in calculations of defect-core structure: Need quantum-mechanical accuracy!

Introduction – Defective crystals

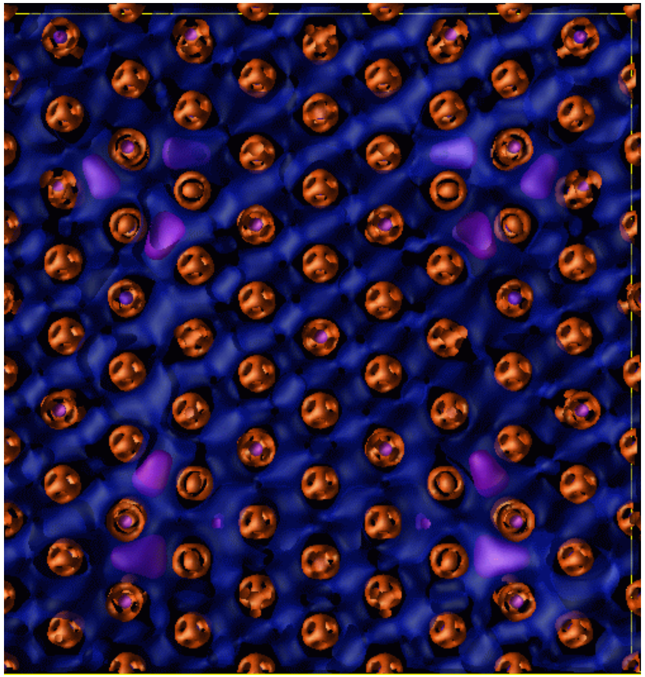

Ab initio study of screw dislocations in Mo and Ta (S. Ismail-Beigi and T. Arias, *Phys. Rev. Let*. **84** (2000) 1499).

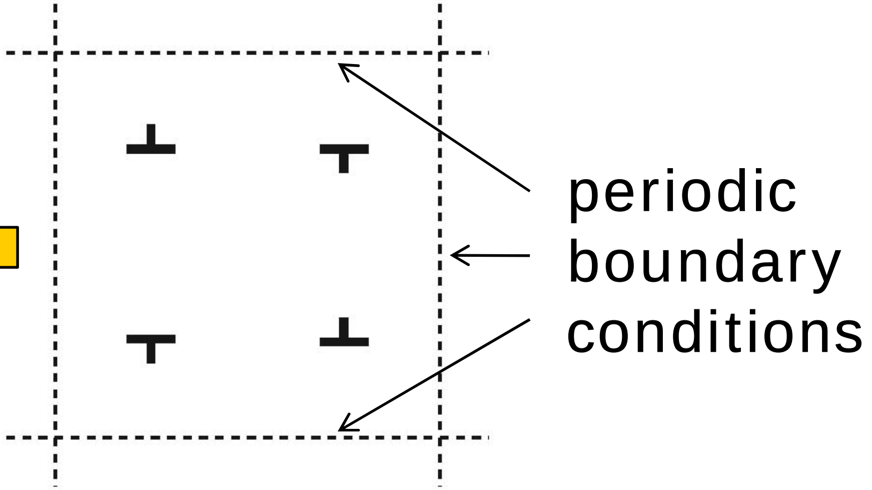

quadrupole arrangement

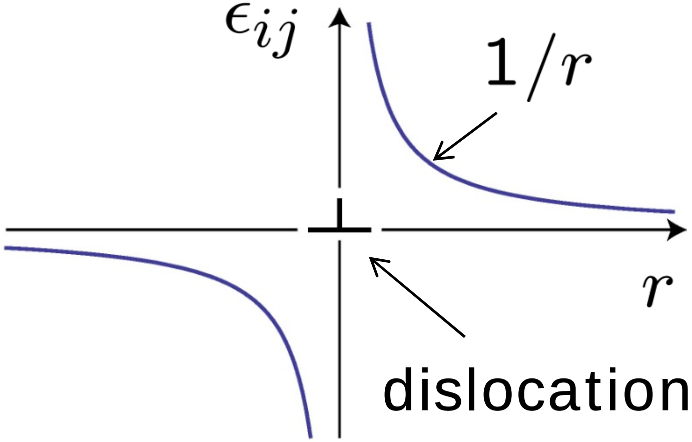

Introduction – Defective crystals

The elastic fields of lattice defects are extremely long ranged. Need large cell sizes to represent physically relevant defect concentrations!

Introduction (QM2CM)

- Problems arising in the study of defective crystals are inherently *multiscale*
- Need to resolve simultaneously:
  - *Electronic structure of defect cores*
  - *Long-range elastic field at physically relevant defect concentrations*
- Typical defect concentrations, cell-size requirements:
  - *Vacancies: cell size* ~ 100 nm
  - *Dislocation cores: cell size* ~ 100 nm
  - *Domain walls: cell size* ~ 1 μm
  - *Grain boundaries: cell size* ~ 20 μm
- Physically relevant cell sizes are far larger than can be analyzed by conventional computational chemistry

Introduction (QM2CM)

Fundamental challenge: Quantum mechanical calculations at macroscopic scales!

Introduction (QM2CM)

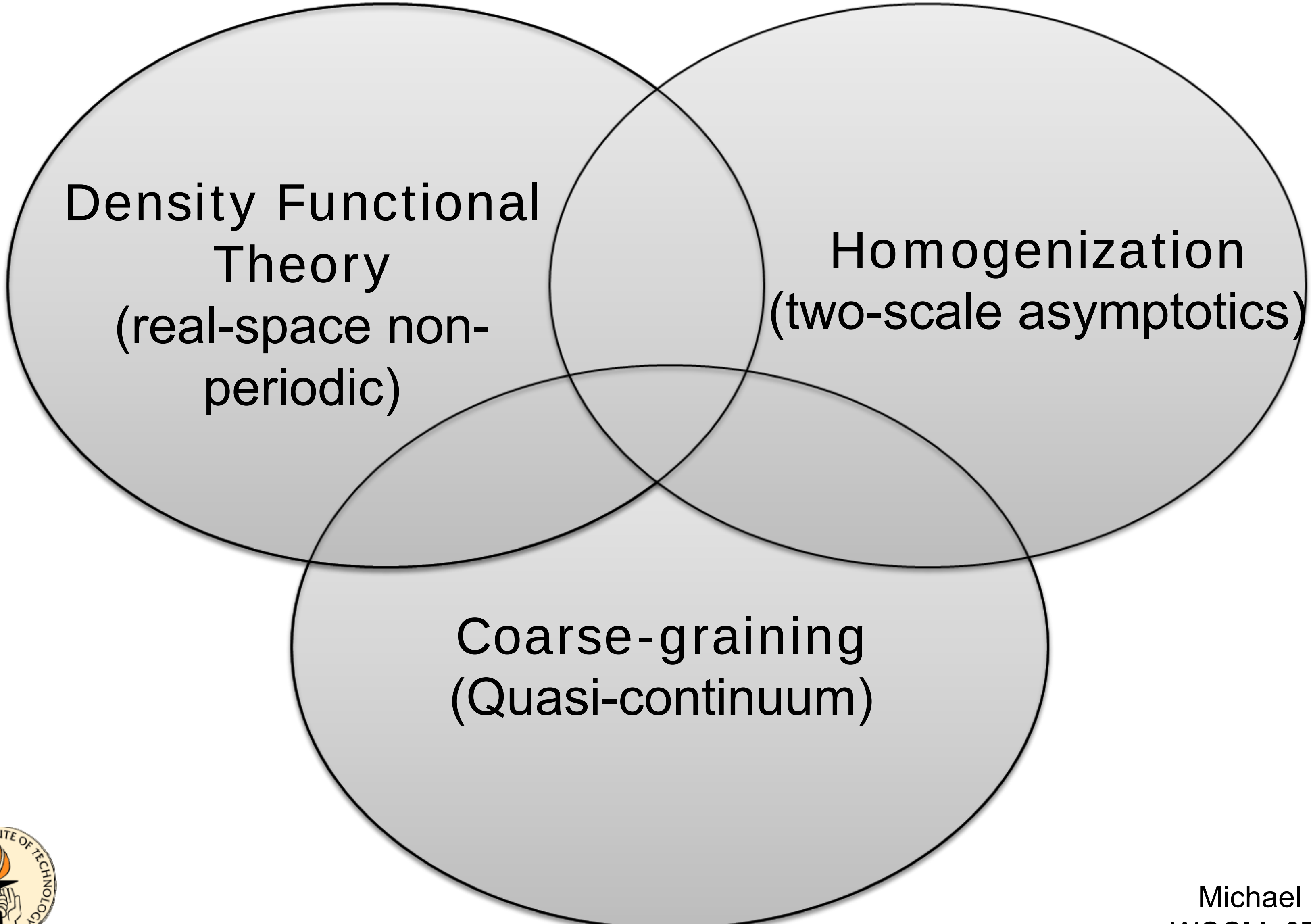

Introduction (QM2CM)

Million-atom electronic structure calculations!

Density Functional Theory

- Theorem [**Hohenberg-Kohn**, 1964] *The external potential* $v(\boldsymbol{r})$ *is determined by the ground state electron density*

$$\rho(\boldsymbol{r}) = N \int |\Psi|^2 ds_1 d\boldsymbol{x}_1 \dots \boldsymbol{x}_N$$

- Levy's constrained-search representation:

$$E[\rho] = \inf_{\Psi \to \rho} \langle \Psi | \widehat{T} + \widehat{V}_{ne} + \widehat{V}_{ee} | \Psi \rangle$$

- Theorem [**Hohenberg-Kohn**, 1964] $E_0 = \inf_\rho E[\rho]$

- $E[\rho]$ not known explicitly! $\Rightarrow$ Model $E[\rho]$

Orbital-Free Density Functional Theory

- Total energy functional: $E[\rho] = T_s[\rho] + E_{xc}[\rho]$

$$+\frac{1}{2}\int_\Omega\int_\Omega \frac{\rho(\boldsymbol{r})\rho(\boldsymbol{r}')}{|\boldsymbol{r}-\boldsymbol{r}'|}\,d\boldsymbol{r}\,d\boldsymbol{r}' + \int \rho(\boldsymbol{r})v(\boldsymbol{r})\,d\boldsymbol{r}$$

- Thomas-Fermi-Weizsacker (TF-λW) KE:

$$T_s(\rho) \approx \frac{3}{10}(3\pi^2)^{2/3}\int \rho^{5/3}(\boldsymbol{r})d\boldsymbol{r} + \frac{\lambda}{8}\int \frac{|\nabla\rho(\boldsymbol{r})|^2}{\rho(\boldsymbol{r})}d\boldsymbol{r}$$

- Exchange-correlation energy (LDA):

$$E_{xc}[\rho] \approx \int \epsilon_c(\rho)\rho(\boldsymbol{r})\,d\boldsymbol{r} - \frac{3}{4}\left(\frac{3}{\pi}\right)^{1/3}\int \rho^{4/3}(\boldsymbol{r})d\boldsymbol{r}$$

Orbital-Free Density Functional Theory

- Total energy functional:

$$E[\rho, \boldsymbol{R}] = \underbrace{\int \epsilon_{loc}(\boldsymbol{r}, \rho, \nabla\rho)\, d\boldsymbol{r}}_{\text{finely oscillatory!}} + \underbrace{\frac{1}{2}\int_\Omega \int_\Omega \frac{\rho(\boldsymbol{r})\rho(\boldsymbol{r}')}{|\boldsymbol{r}-\boldsymbol{r}'|}\, d\boldsymbol{r}\, d\boldsymbol{r}'}_{\text{nonlocal!}}$$

- Local Lagrangian form: $E[\rho, \boldsymbol{R}] = \sup\limits_{\phi \in H^1(\mathbf{R}^3)} L[\rho, \phi, \boldsymbol{R}]$

$$L[\rho, \phi, \boldsymbol{R}] = \int \epsilon_{loc}(\boldsymbol{r}, \rho, \nabla\rho)\, d\boldsymbol{r}$$

$$-\frac{1}{8\pi}\int_\Omega |\nabla\phi(\boldsymbol{r})|^2\, d\boldsymbol{r} + \int_\Omega (\rho(\boldsymbol{r}) + \underbrace{b(\boldsymbol{r})}_{\text{pseudopotentials}})\phi(\boldsymbol{r})\, d\boldsymbol{r}$$

Orbital-Free Density Functional Theory

'Garden-variety' functionals amenable to standard finite-element discretization!

OFDFT – Fully resolved FE

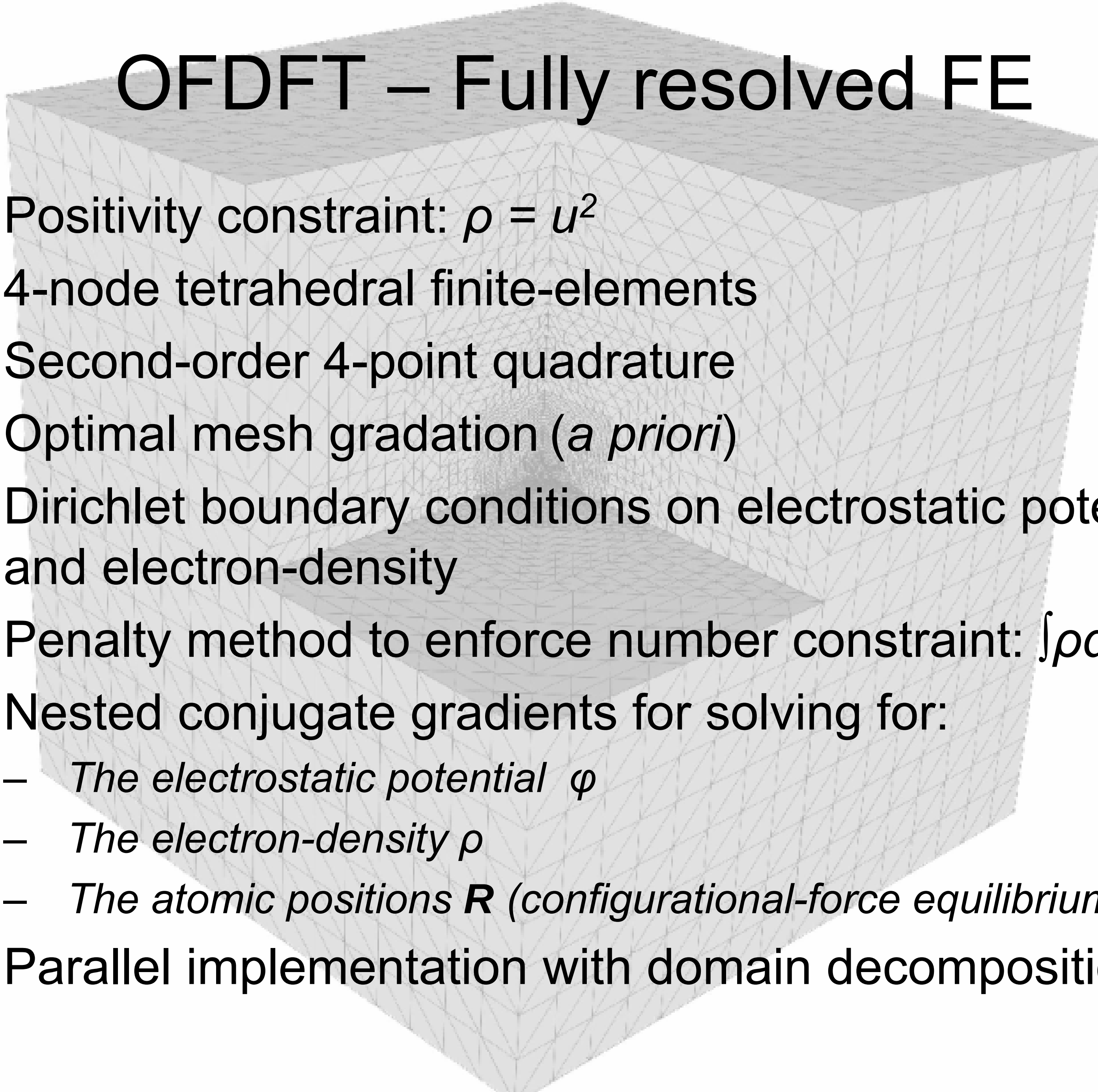

- Positivity constraint: $\rho = u^2$
- 4-node tetrahedral finite-elements
- Second-order 4-point quadrature
- Optimal mesh gradation (*a priori*)
- Dirichlet boundary conditions on electrostatic potential and electron-density
- Penalty method to enforce number constraint: $\int \rho dx = N$
- Nested conjugate gradients for solving for:
  - *The electrostatic potential* φ
  - *The electron-density* ρ
  - *The atomic positions* $\mathbf{R}$ *(configurational-force equilibrium)*
- Parallel implementation with domain decomposition

Convergence test – Hydrogen atom

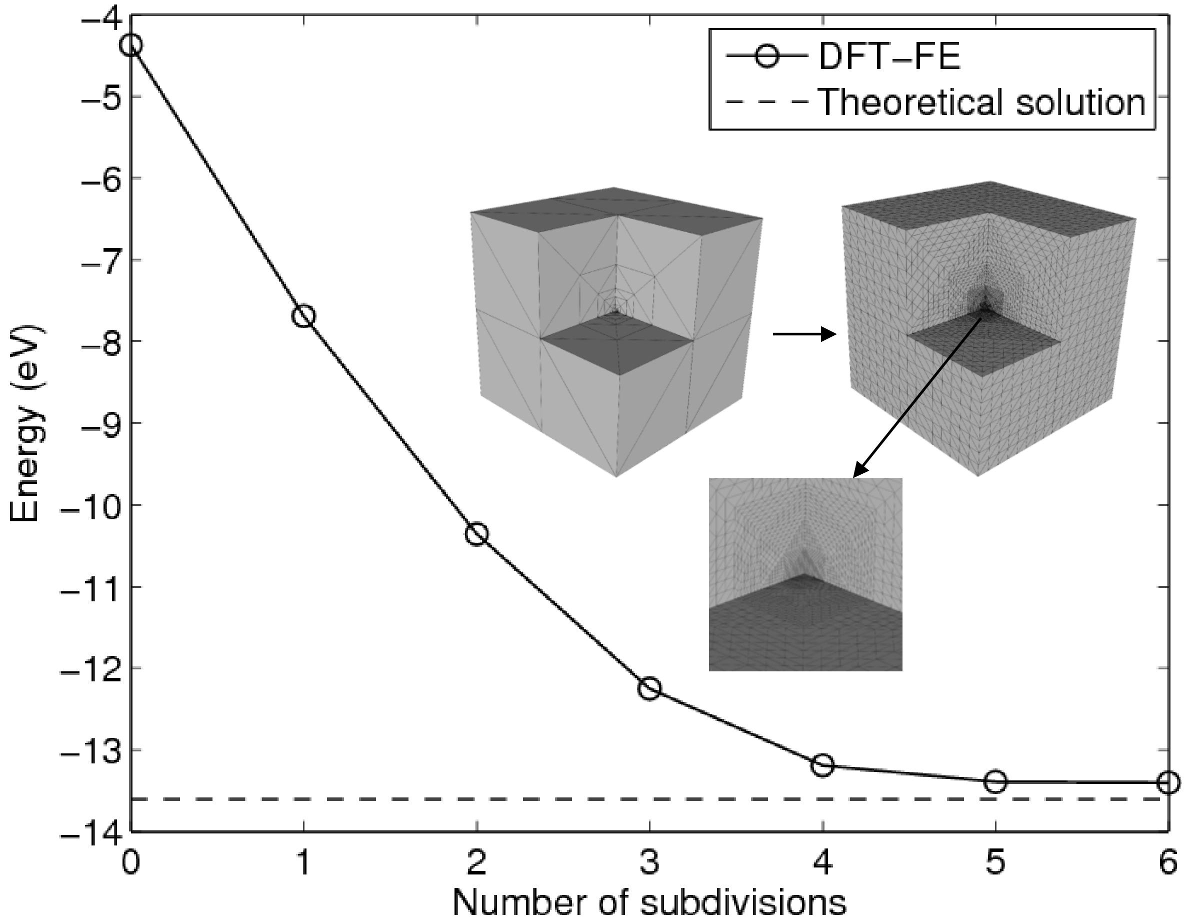

Energy of hydrogen atom as a function of number of subdivisions of initial mesh

Example – Aluminum nanoclusters

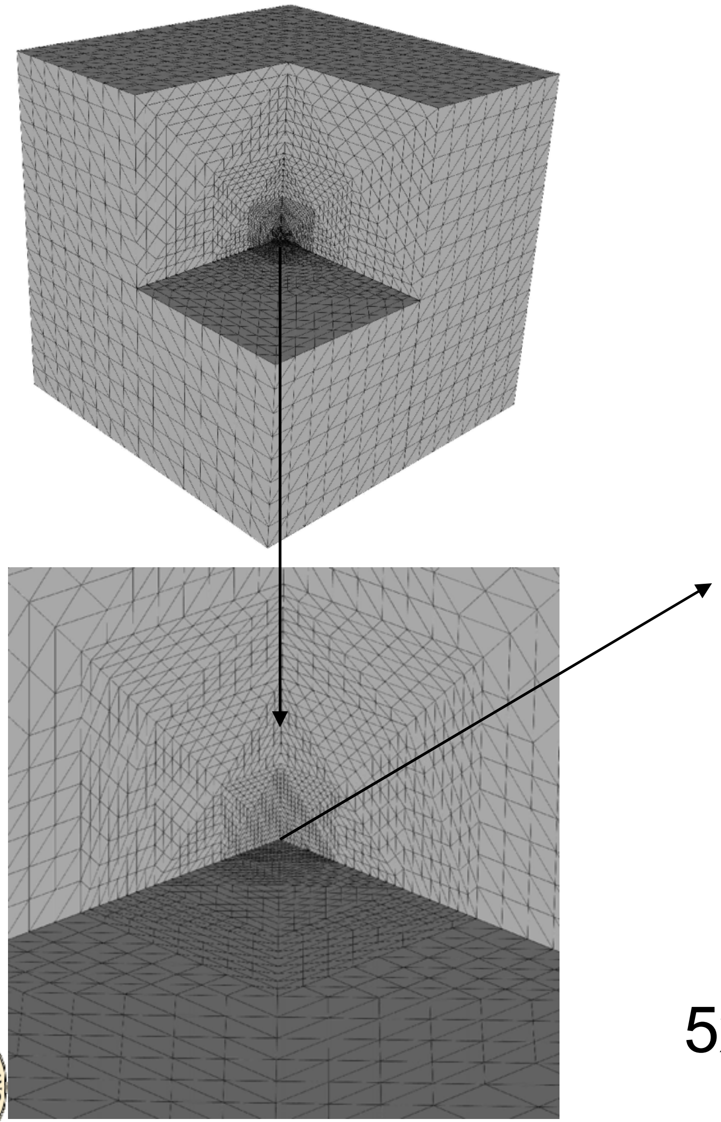

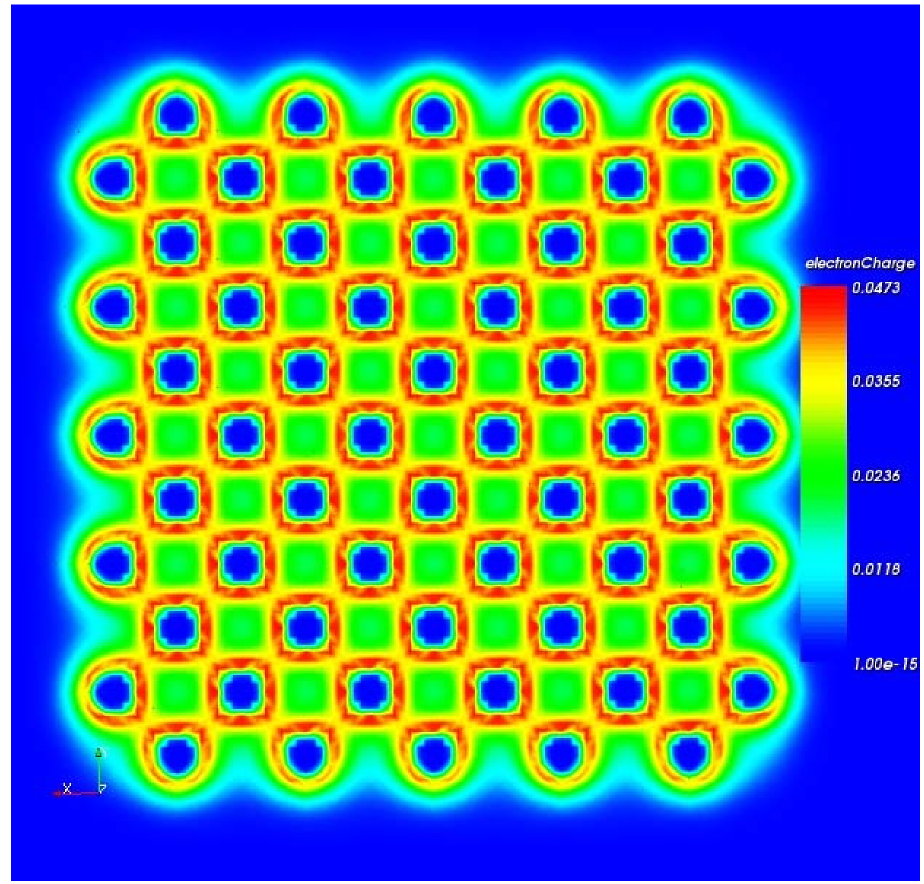

Contours of electron density in 5x5x5 aluminum cluster (mid plane)

Michael Ortiz
WCCM 07/01/08

Example – Aluminum nanoclusters

Property	DFT-FE	KS-LDA[a]	Experiments[b]
Lattice parameter (a.u.)	7.42	7.48	7.67
Cohesive energy (eV)	3.69	3.67	3.4
Bulk modulus (Gpa)	83.1	79.0	74.0

a/ Goodwin et al. (1990), Gaudion et al. (2002)

b/ Brewer (1997), Gschneider (1964)

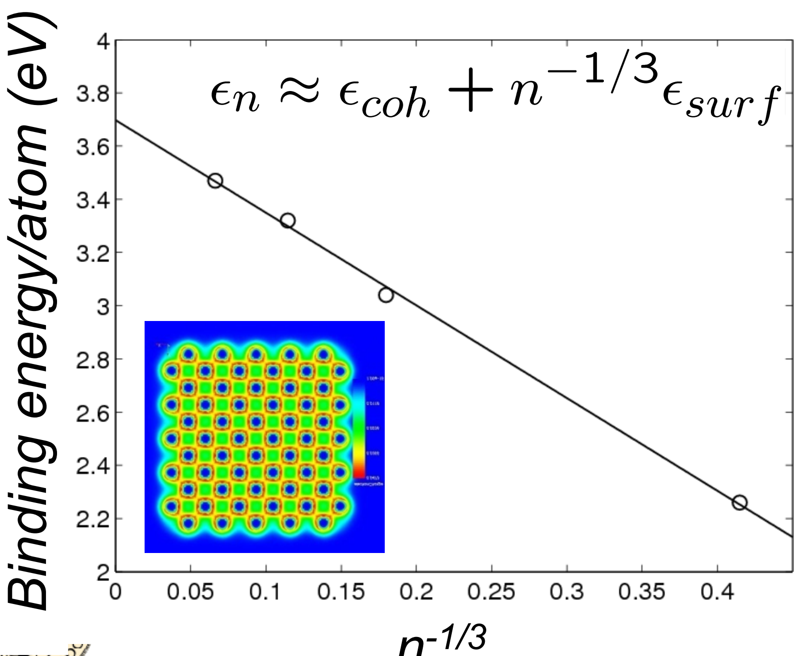

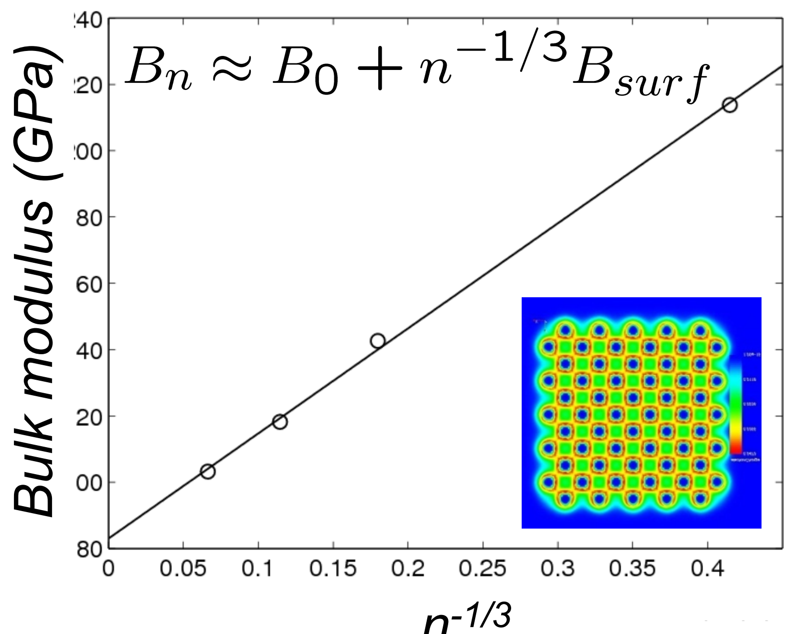

OFDFT – Coarse-graining

- Real-space formulation and finite-element approximation → Nonperiodic, unstructured, OFDFT calculations
- However, calculations are still expensive: 9x9x9 cluster = 3730 atoms required 10,000 CPU hours!

Need to homogenize, coarse-grain → Multiscale analysis!

Introduction (QM2CM)

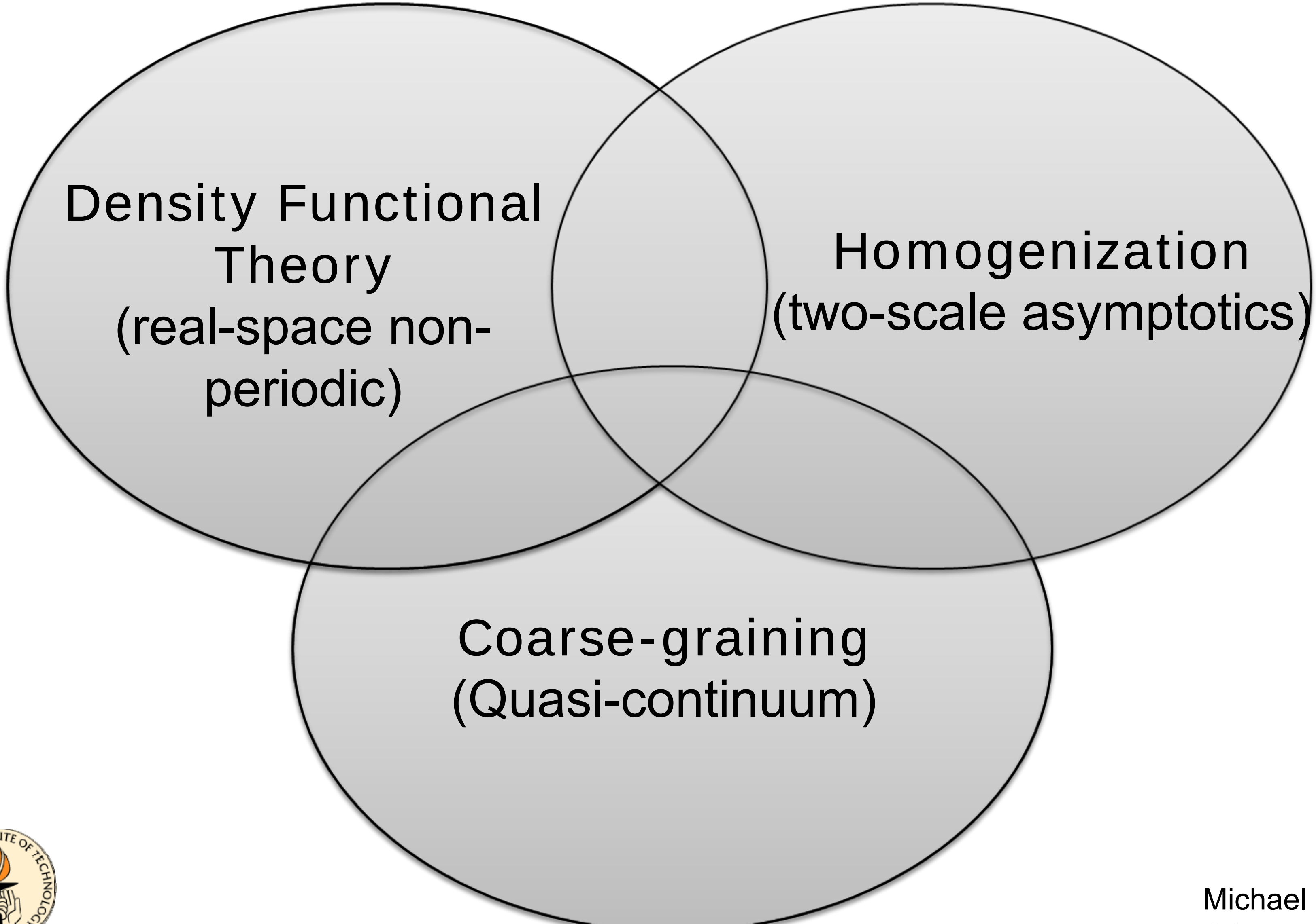

Defective crystals – The bridge

- Away from defects, atoms 'see' the electron density of a uniformly distorted periodic lattice: Cauchy-Born electron density + slowly varying modulation (Blanc, Le Bris and Lions, ARMA, 2002)

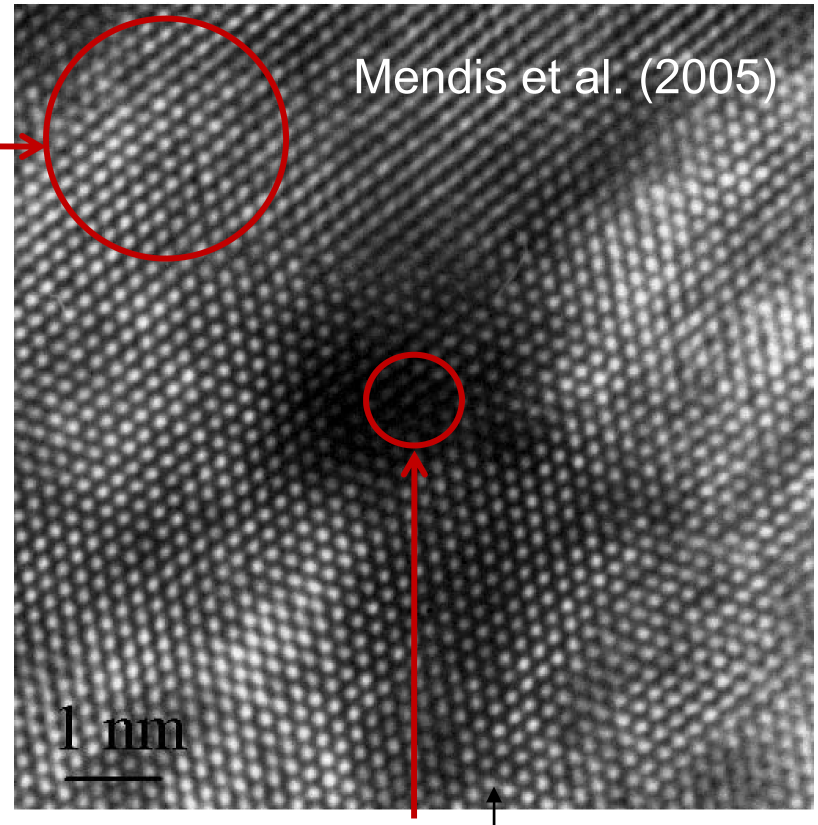

- Only near defect cores the electron density and the electrostatic potential deviate significantly from those of a periodic lattice

Defective crystals – The bridge

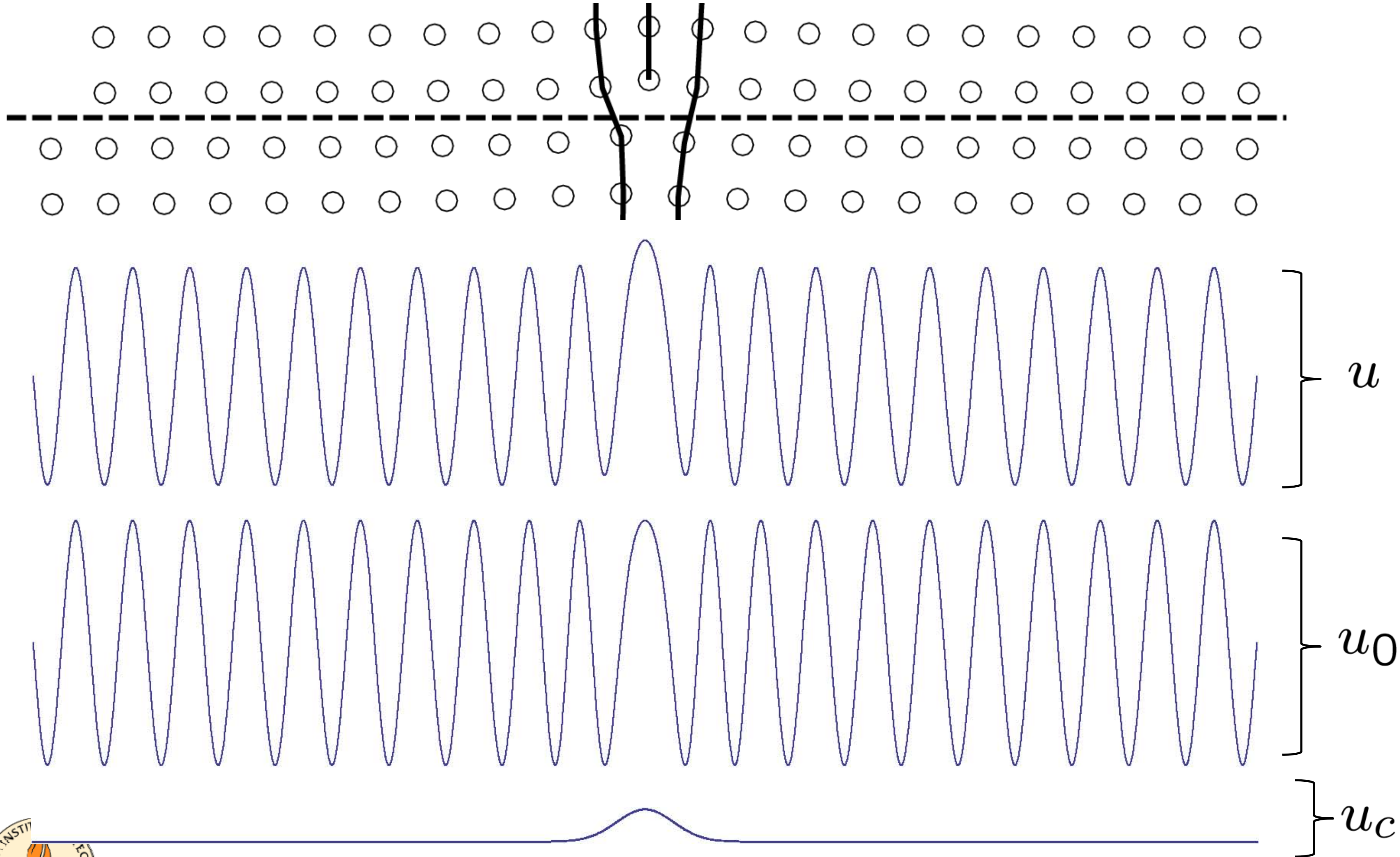

$$u \sim u_0 + u_c$$

QC/OFDFT – Multiscale hierarchy

- Quasi-continuum: $\boldsymbol{R} \to \boldsymbol{R}_h \in \mathbb{R}^{3N_h}, \quad N_h \ll N$

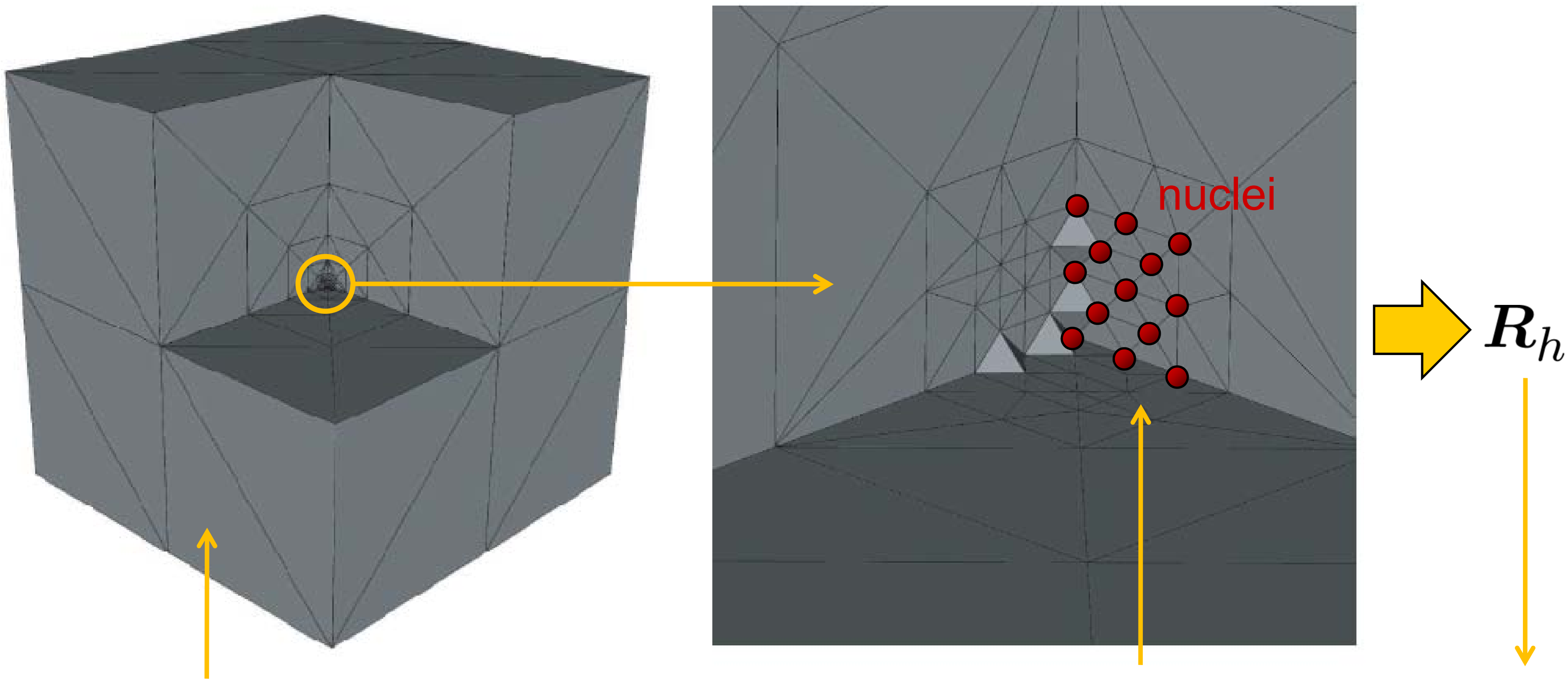

coarse resolution, nuclei in interpolated positions

atomic resolution, nuclei in arbitrary positions

relaxed nuclei

QC/OFDFT – Multiscale hierarchy

- Each element represents affinely deformed lattice

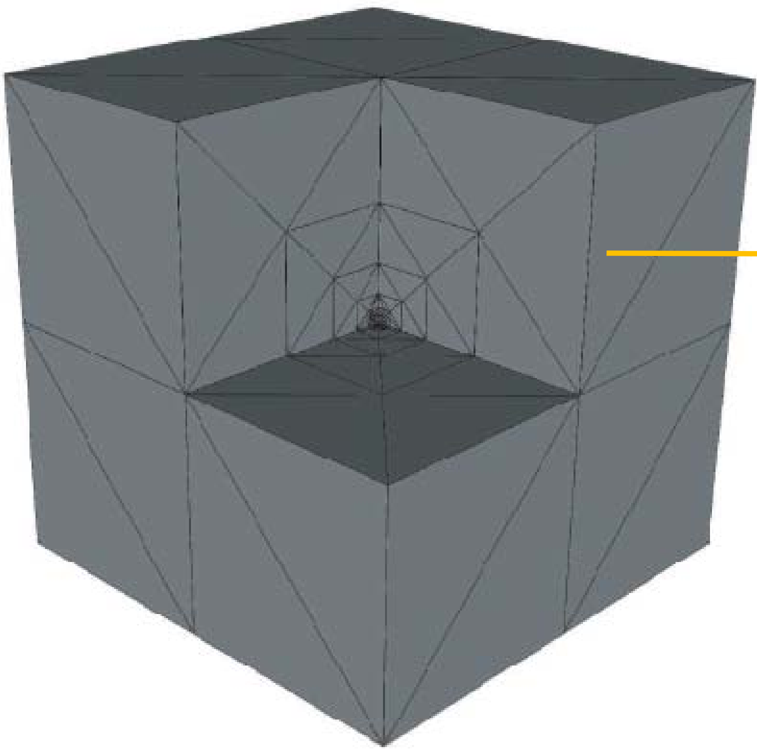

QC mesh, nuclei in interpolated positions

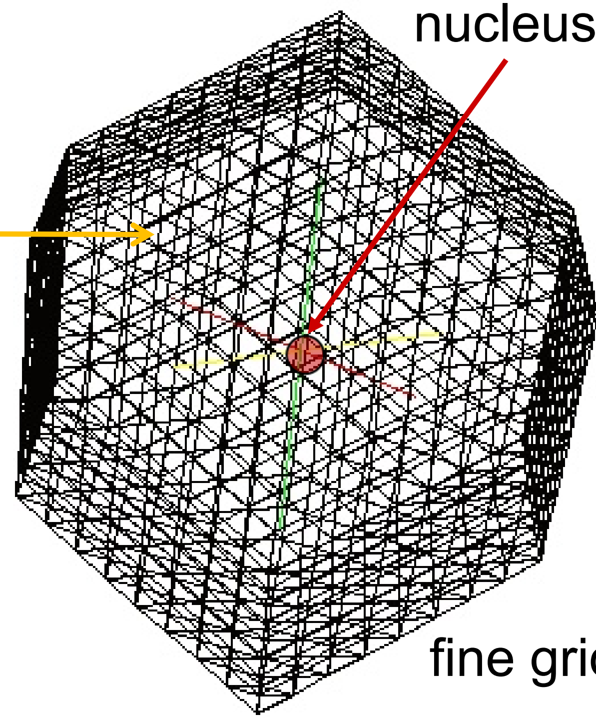

unit cell calculation, affinely deformed lattice

$$\Rightarrow \begin{cases} \rho_h^0 \\ \phi_h^0 \end{cases}$$

Cauchy-Born predictor

QC/OFDFT – Multiscale hierarchy

- Localized correction to Cauchy-Born predictor:

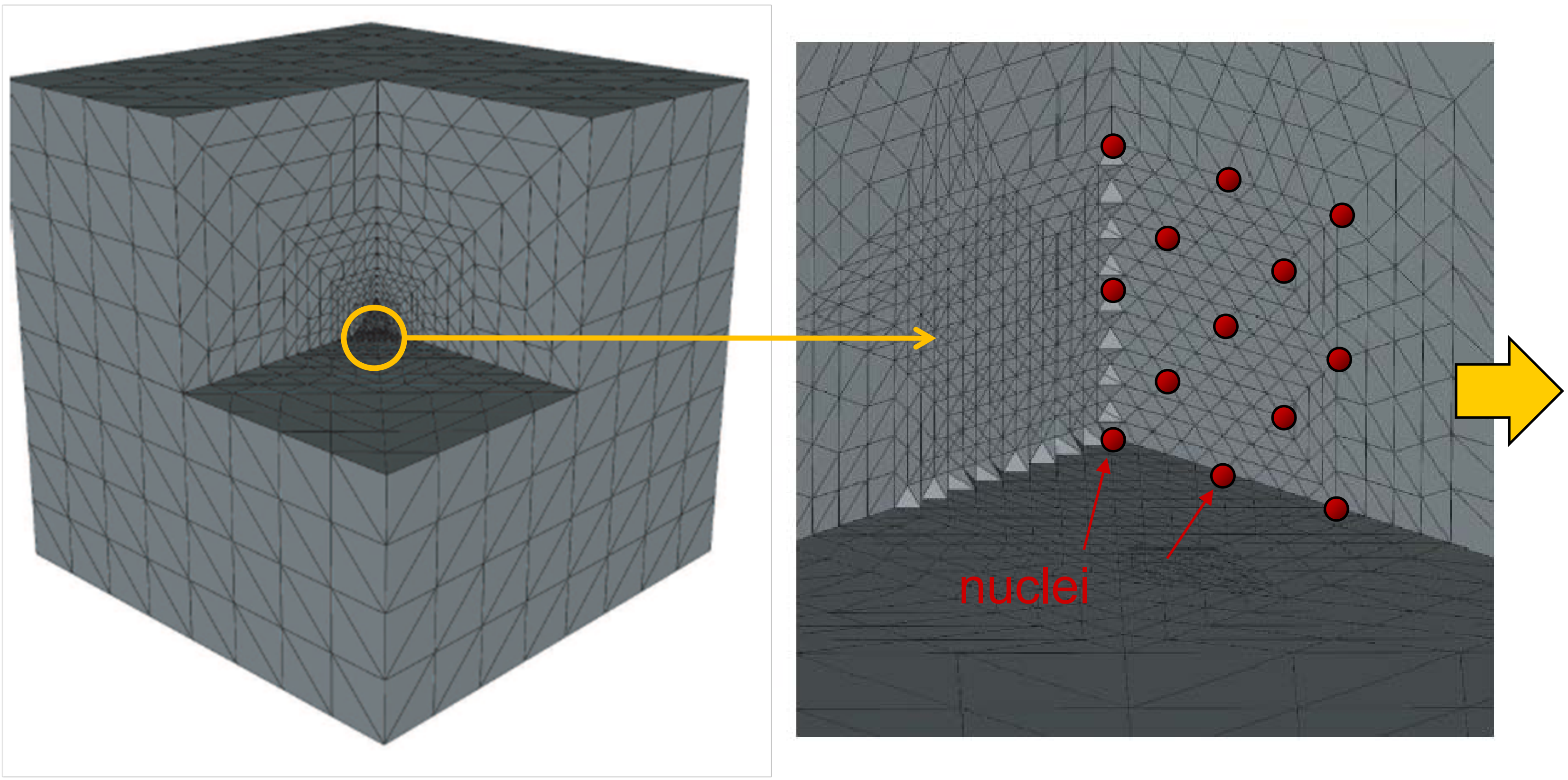

$$\begin{cases} \rho_h^c \\ \phi_h^c \end{cases}$$

coarse mesh
macroscopic resolution

fine mesh
subatomic resolution

localized
correction

QC/OFDFT – Attributes

- The overall complexity of the method is set by the size of the intermediate mesh (interpolation of ρ_c, φ_c)
- All approximations are numerical: interpolation of fields, numerical quadrature
- No spurious physics is introduced: OFDFT is the sole input to the model
- A converged solution obtained by this scheme is a solution of OFDFT
- Coarse graining is seamless, unstructured, adaptive: no periodicity, no interfaces
- Fully-resolved OFDFT and continuum finite elasticity are obtained as extreme limits

QC/OFDFT – Attributes

Million-atom OFDFT calculations possible at no significant loss of accuracy!

QC/OFDFT convergence – Al vacancy

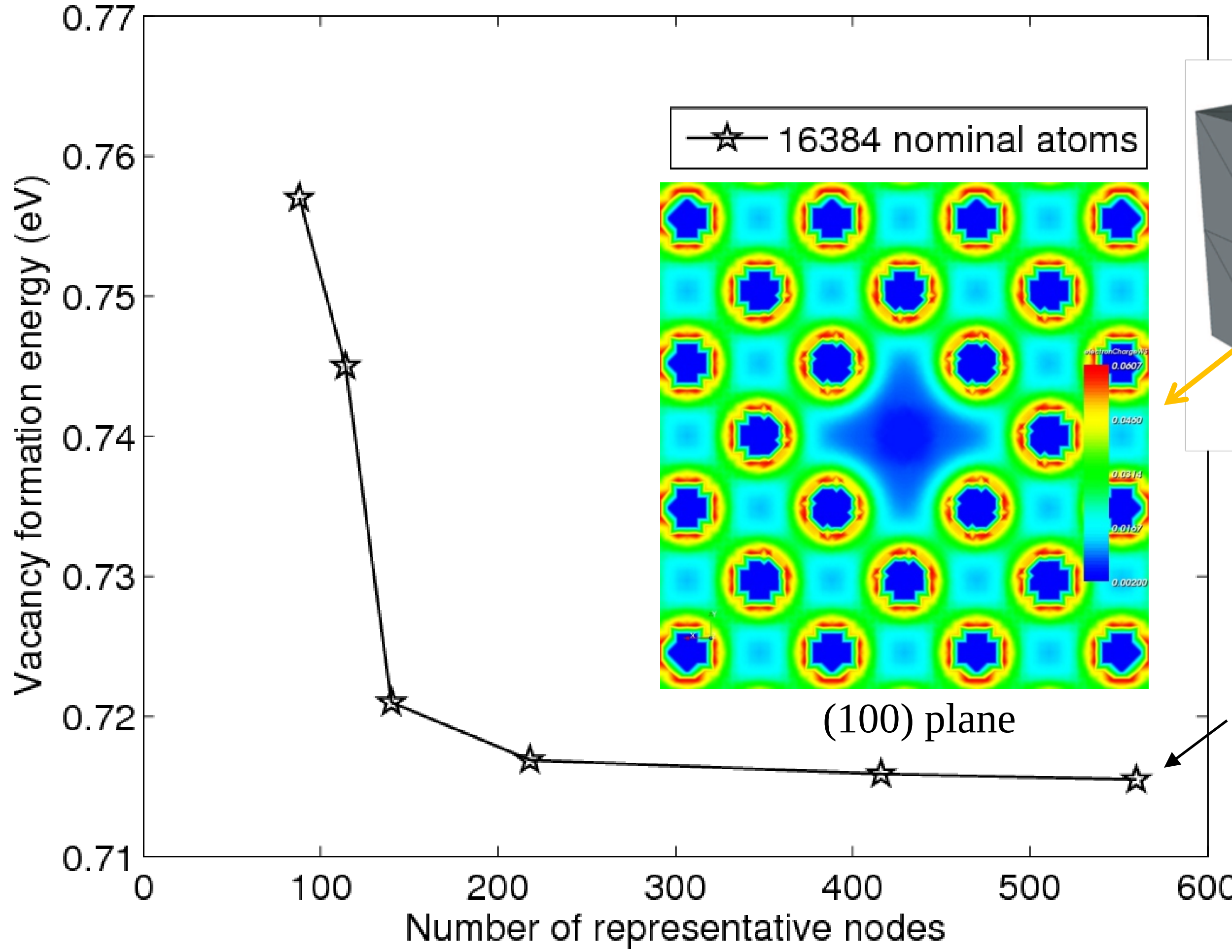

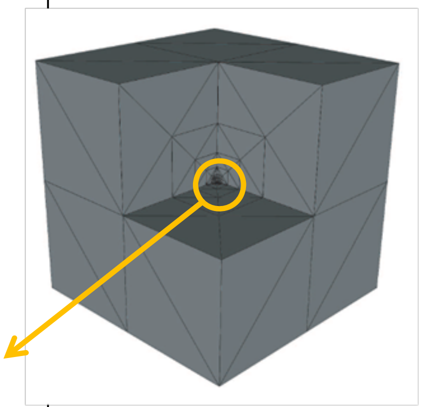

4% of nuclei accounted for in calculation at no loss of accuracy!

Convergence of multiscale scheme

Michael Ortiz
WCCM 07/01/08

Cell-size dependence – Al vacancy

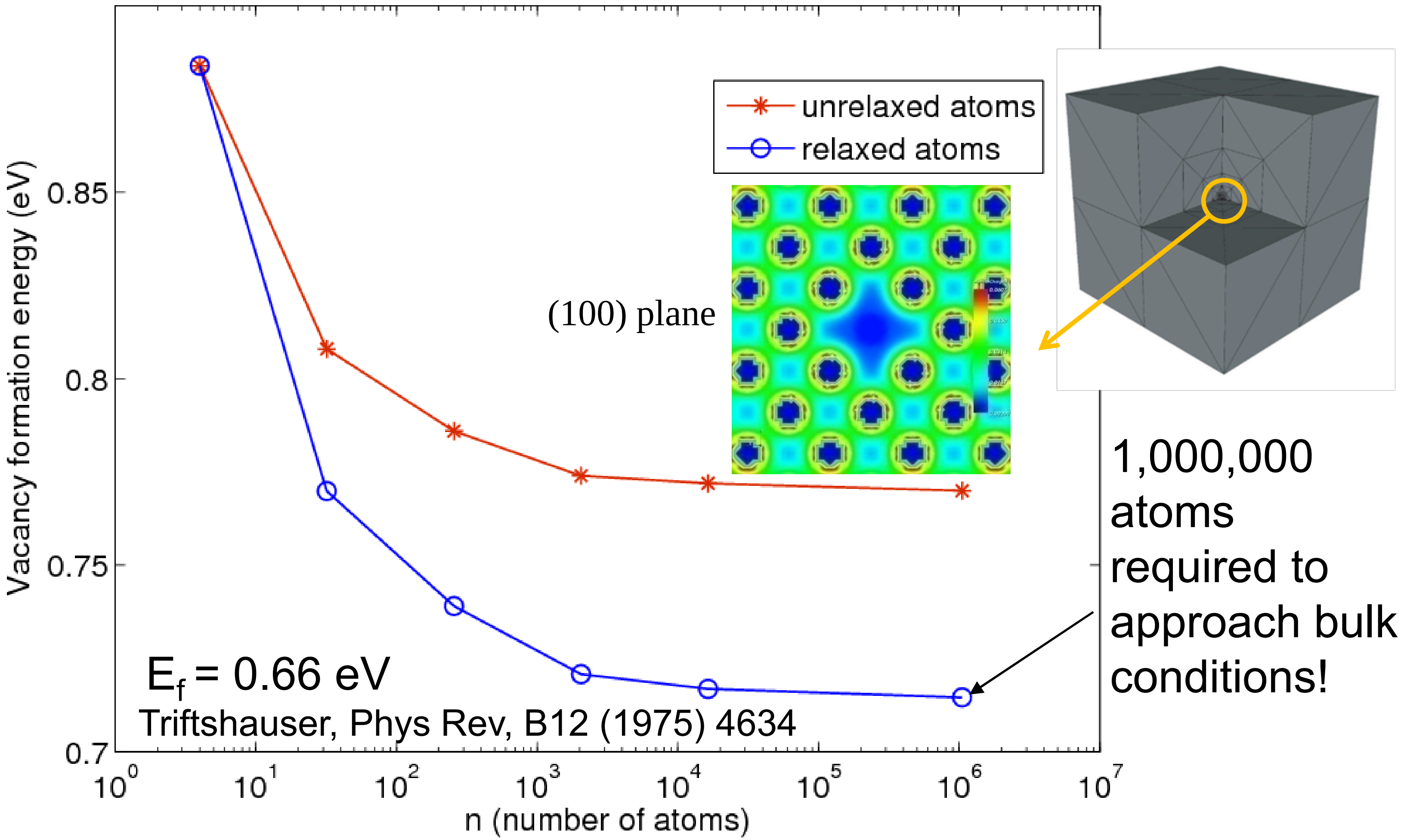

Convergence with material sample size

QC/OFDFT convergence – Al vacancy

- QC reduction converges rapidly:
  - *16,384-atom sample: ~200 representative atoms required for ostensibly converged vacancy formation energy.*
  - *1,000,000-atom sample: ~1,017 representative atoms and ~ 450,000 electron-density nodes give vacancy formation energy within ~0.01 eV of converged value*
- Vacancies have long-range elastic field and convergence with respect to sample size is slow: ~1,000,000 atom sample required to attain single-vacancy formation energy!
- What can we learn from large cell sizes?
  - *Case study 1: Di-vacancies in aluminum*
  - *Case studey 2: Prismatic loops in aluminum*

Case study 1 – Di-vacancies in Al

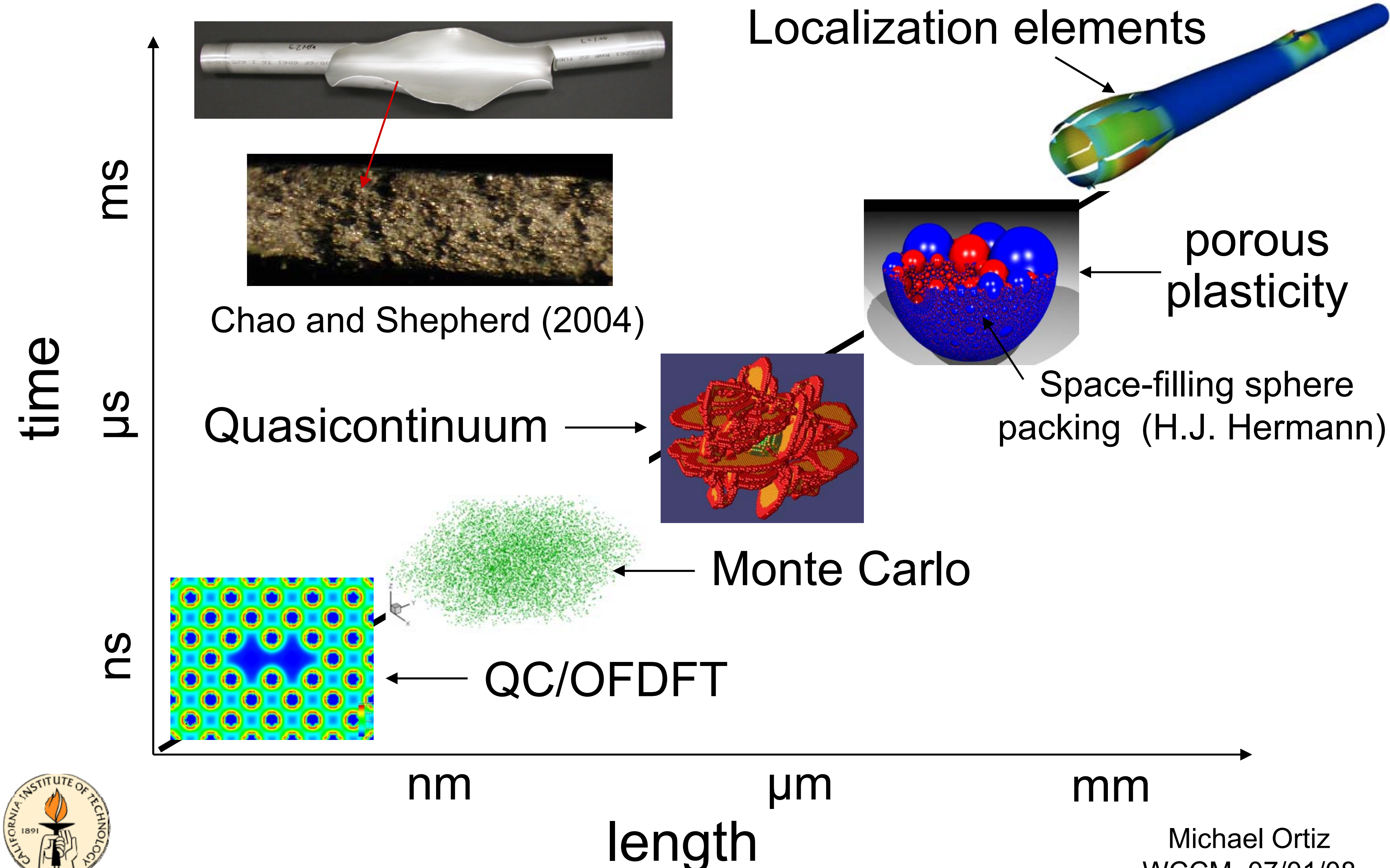

Case study 1 – Di-vacancies in Al

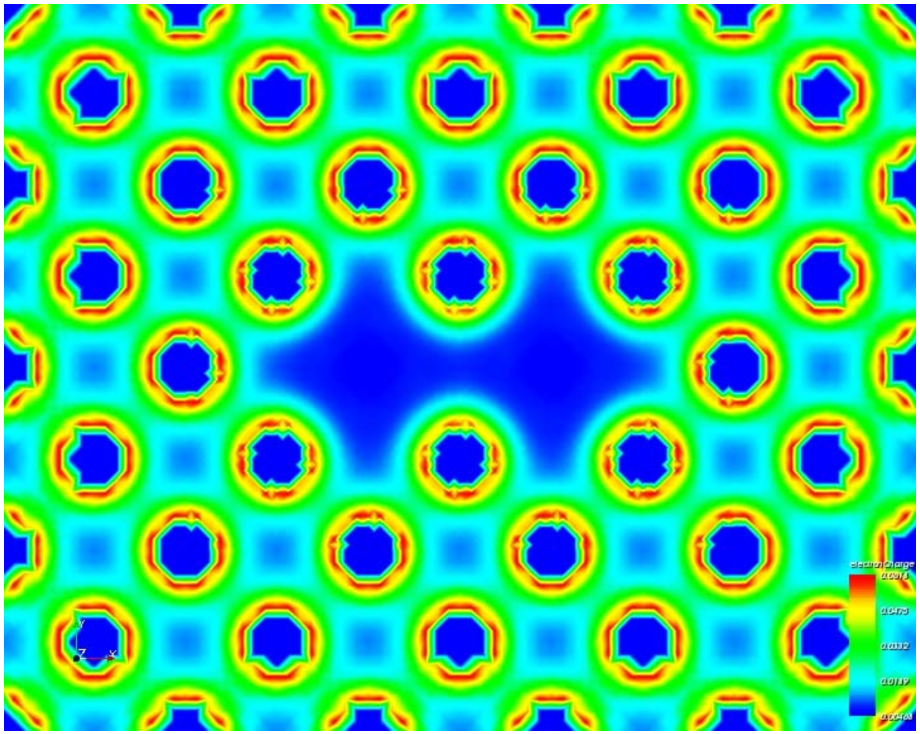

Di-vacancy along <100>

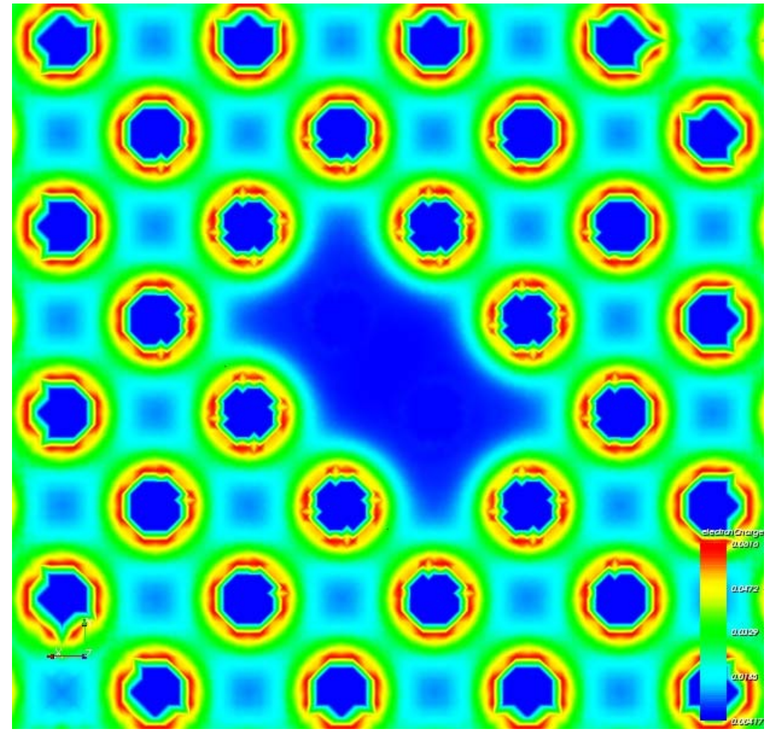

Di-vacancy along <110>

Core electronic structure

Michael Ortiz
WCCM 07/01/08

Case study 1 – Di-vacancies in Al

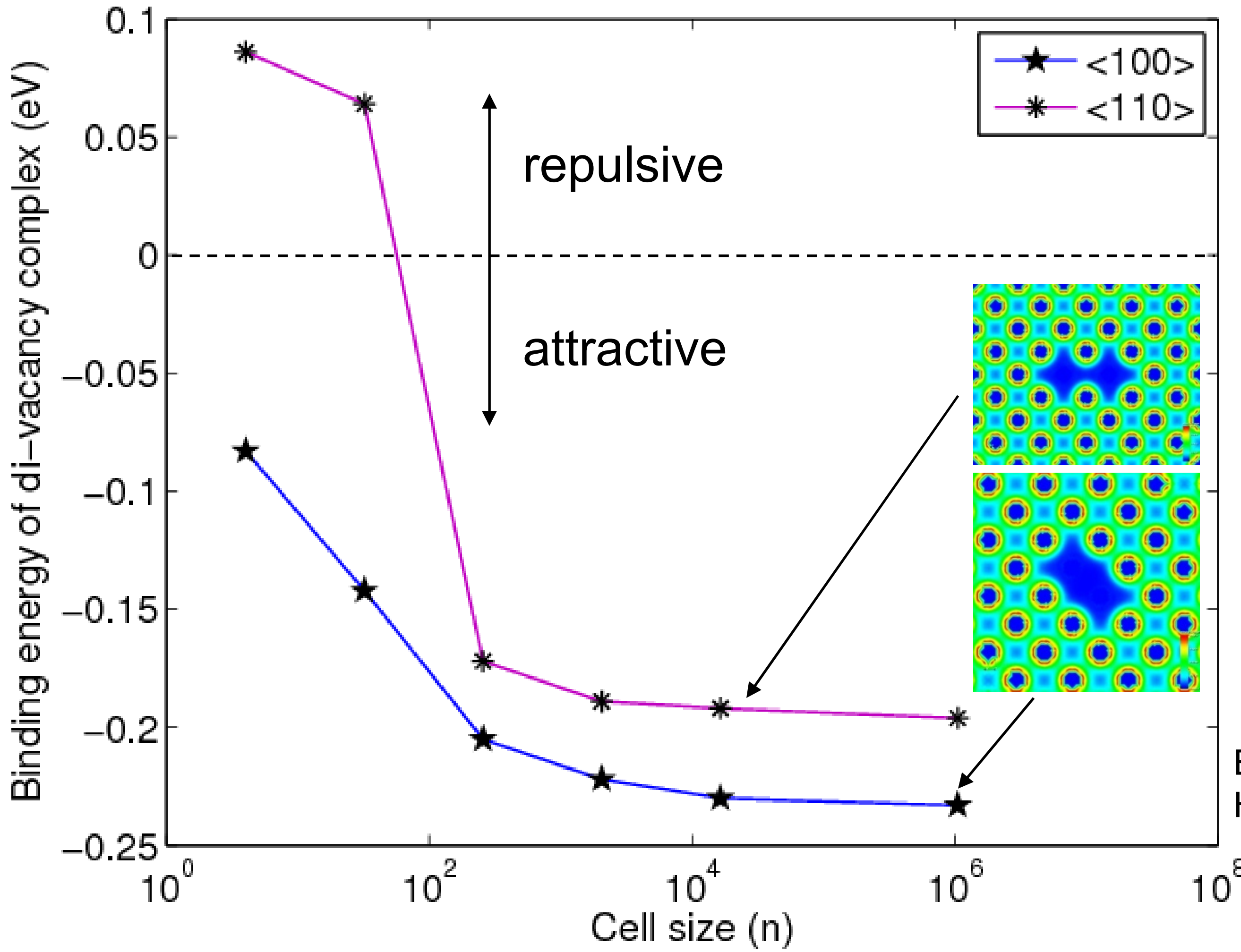

E_f =
-0.2 to
-0.3 eV

Ehrhart et al., 1991
Hehenkamp, 1994

Binding energy *vs.* material sample size

Case study 1 – Vacancies in Al

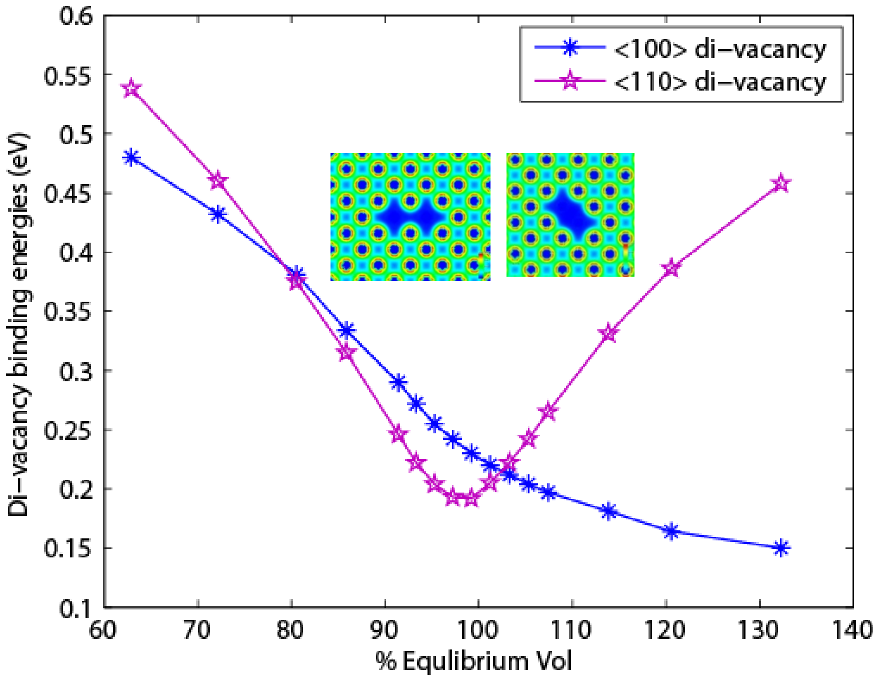

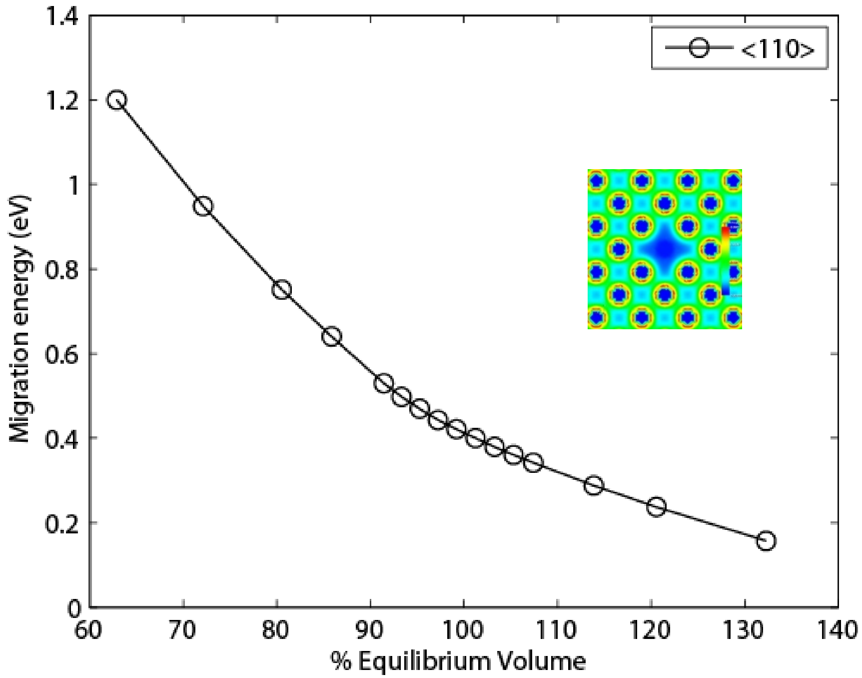

Binding energy *vs.* volume   Migration energy *vs.* volume

Vacancies in shocked aluminum

Michael Ortiz
WCCM 07/01/08

Case study 1 – Vacancies in Al

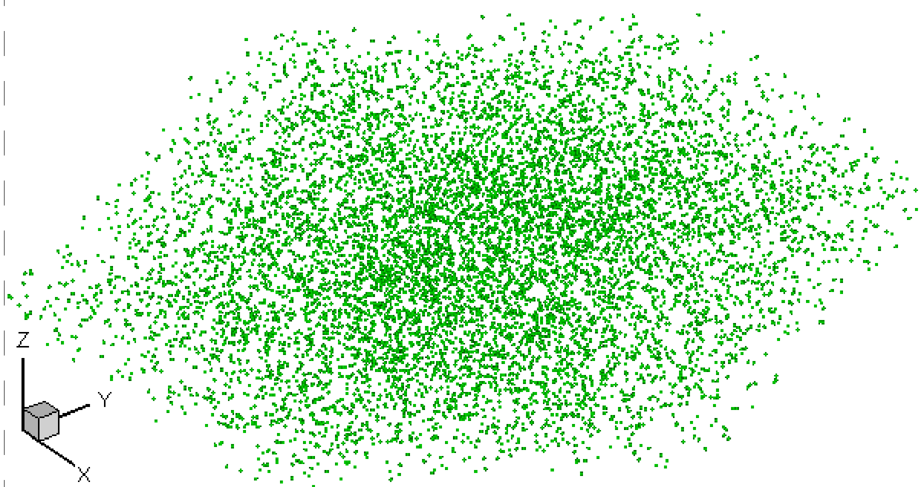

Time evolution of number
of voids of different sizes

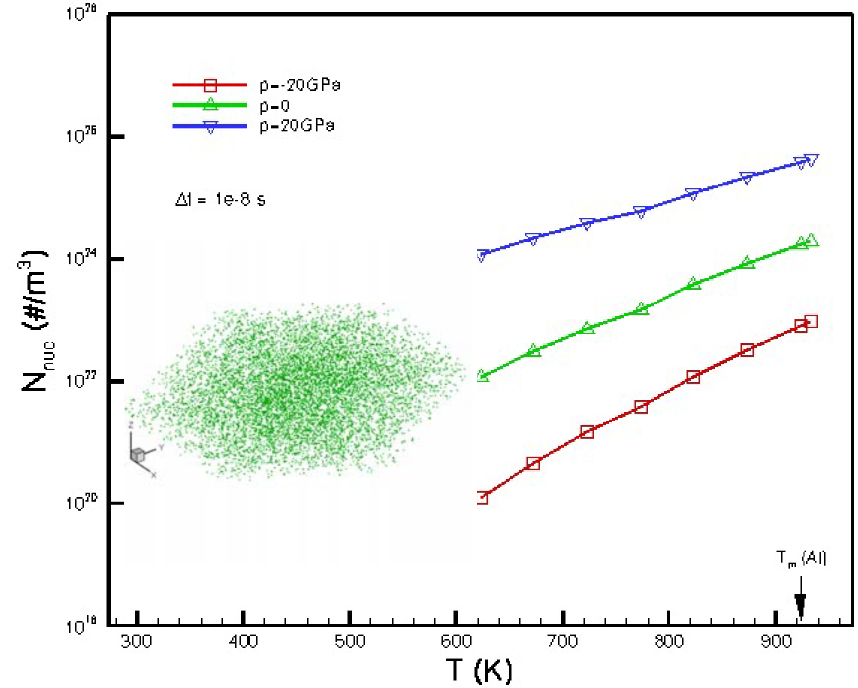

Density of nanovoids (1nm)
nucleated in 10^{-8} s

Nanovoid nucleation in shocked aluminum

Case study 1 – Di-vacancies in Al

- Strong cell-size effect: binding energy changes from repulsive at large concentrations to attractive at bulk concentrations
- Sample sizes containing > 1,000,000 atoms must be used in order to approach bulk conditions
- Di-vacancy binding energies are computed to be:

  -0.19 eV for <110> di-vacancy; -0.23 eV for <100> di-vacancy
- Agreement with experimental values: -0.2 to -0.3 eV (Ehrhart et al., 1991; Hehenkamp, 1994)
- Small-cell size values consistent with previous DFT calculations (Carling et al., 2000; Uesugi et. al, 2003) :

  +0.05 eV for <110> di-vacancy; -0.04 eV for <100> di-vacancy
- No discrepancy between theory and experiment, only strong vacancy-concentration effect!

Case study 2 – Prismatic loops in Al

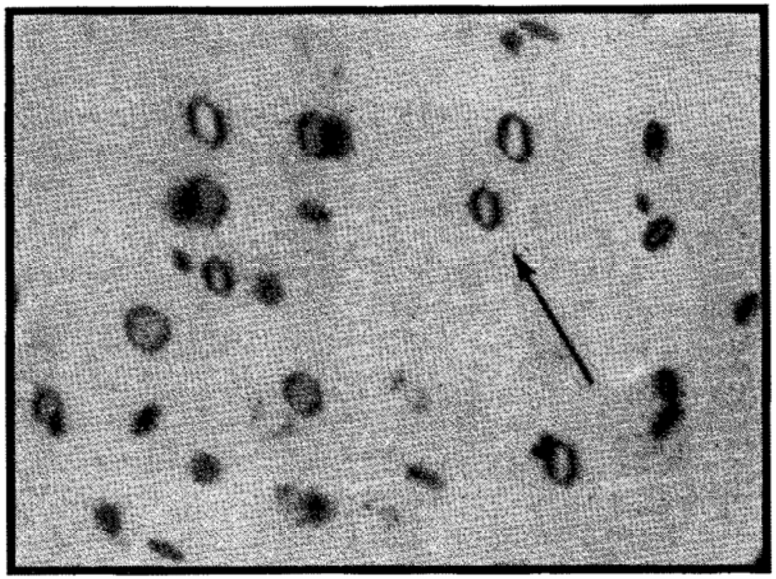

Prismatic dislocation loops formed by condensation of vacancies in quenched aluminum

Kulhmann-Wilsdorff and Kuhlmann, *J. Appl. Phys.*, **31** (1960) 516.

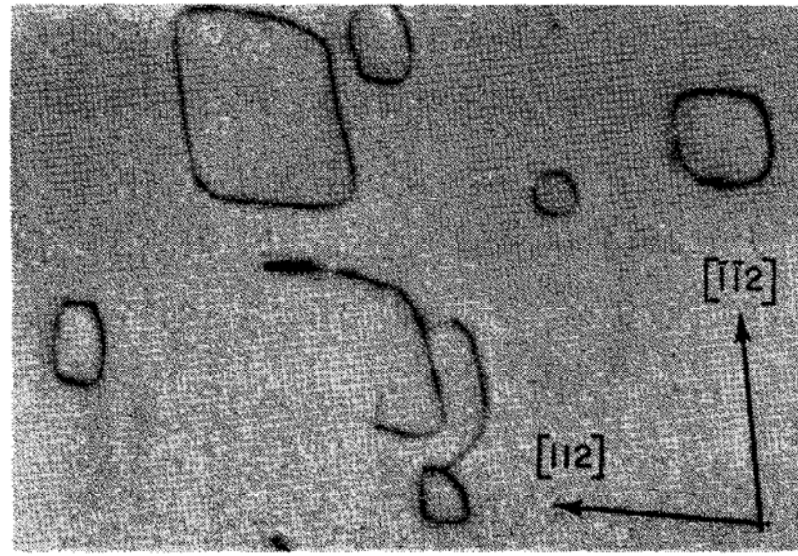

Prismatic dislocation loops formed by condensation of vacancies in quenched Al-05%Mg

Takamura and Greensfield, *J. Appl. Phys.*, **33** (1961) 247.

- Prismatic dislocation loops also in irradiated materials
- Loops smaller than 50 nm undetectable: Nucleation mechanism? Vacancy condensation?

Case study 2 – Prismatic loops in Al

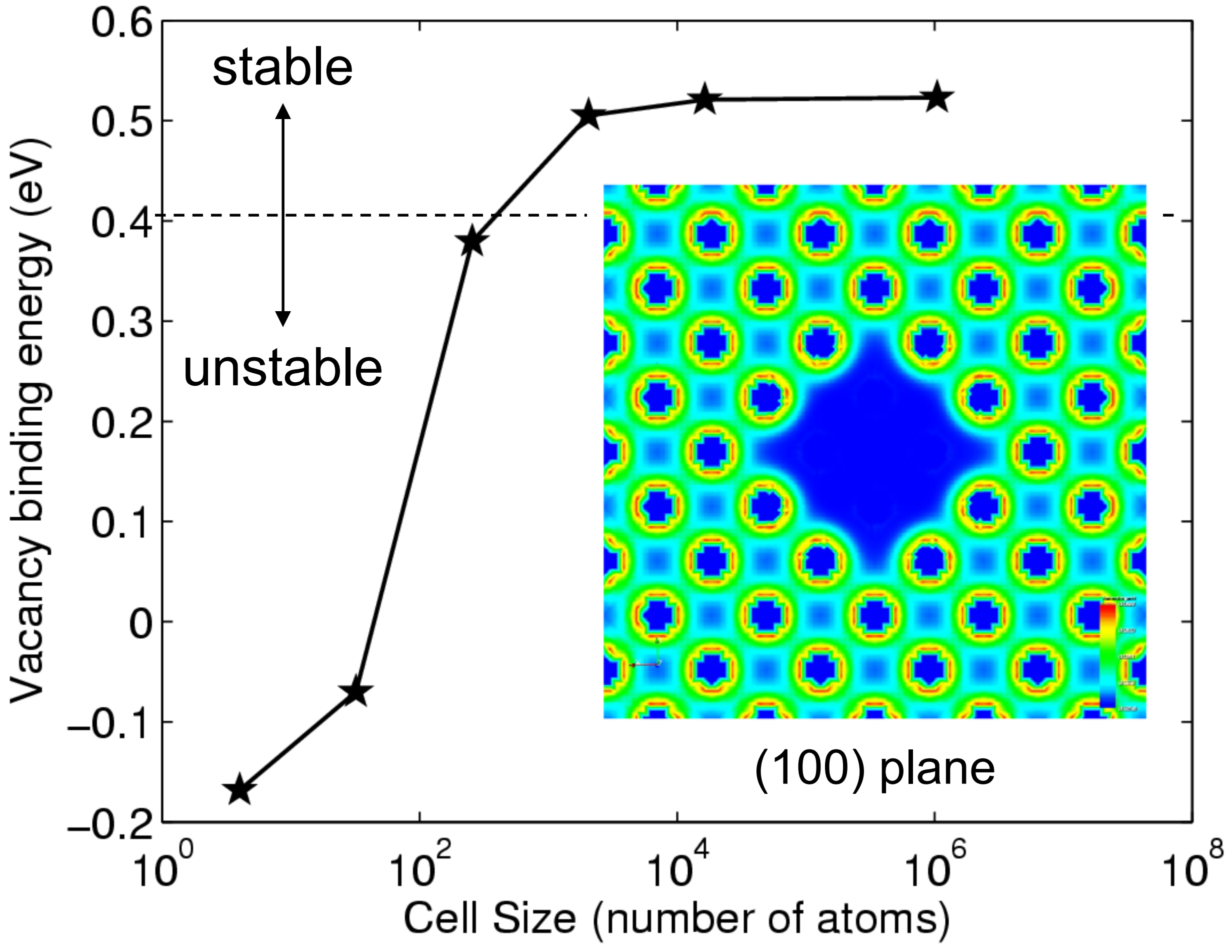

Quad-vacancy binding energy *vs.* material sample size

Michael Ortiz
WCCM 07/01/08

Case study 2 – Prismatic loops in Al

(111)

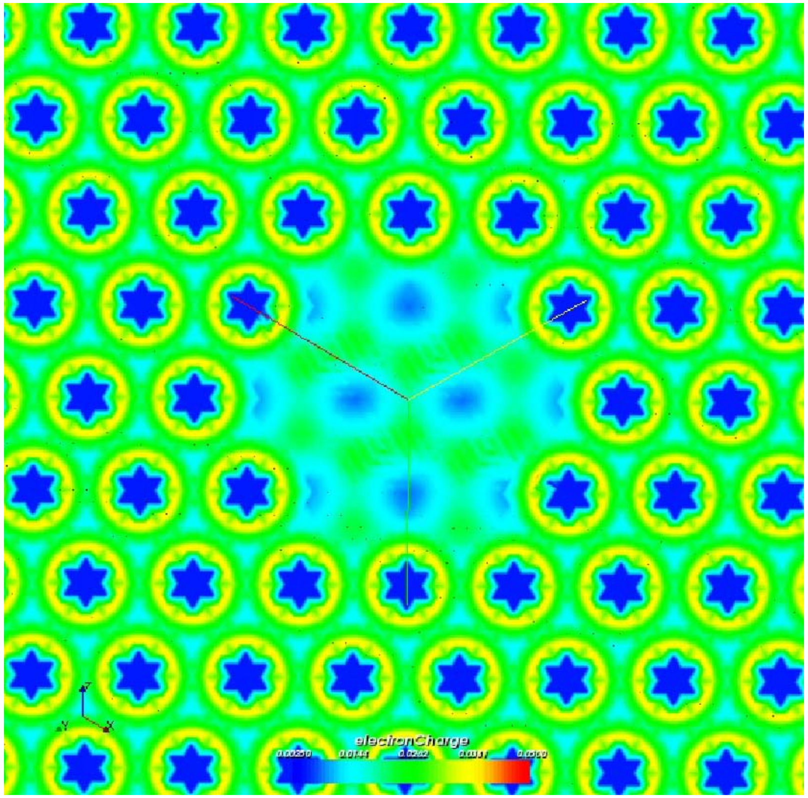

Non-collapsed configuration

Binding energy = -0.88 eV

(001)

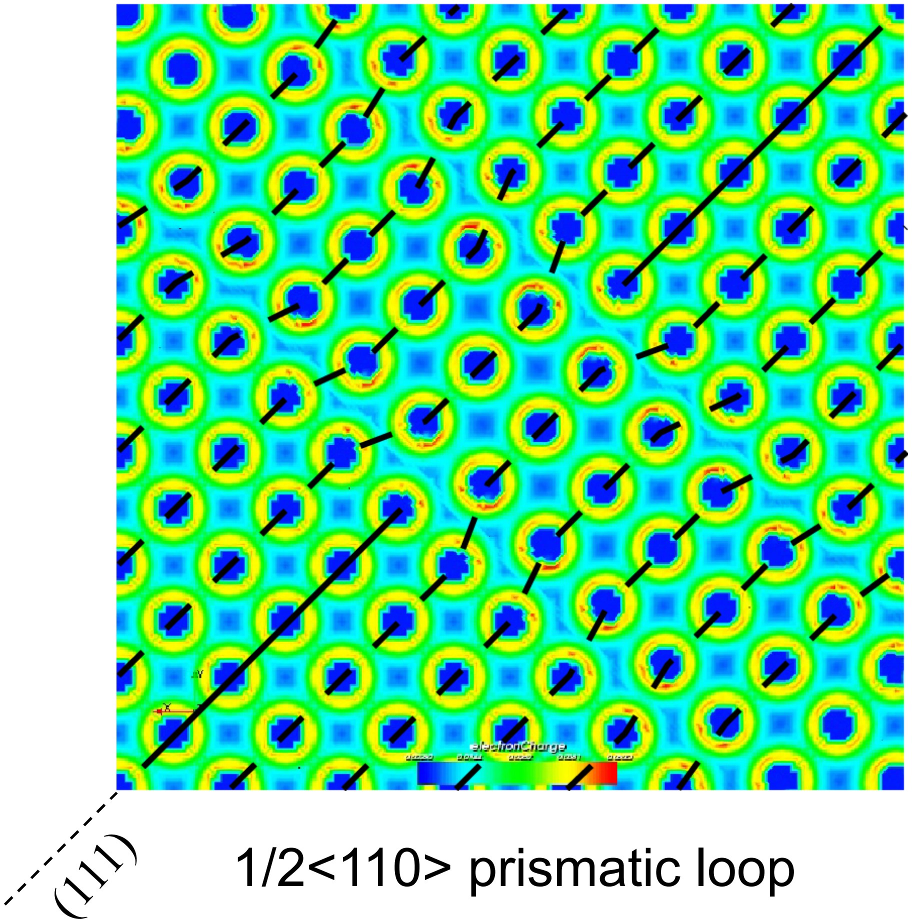

1/2<110> prismatic loop

Binding energy = -1.57 eV

Stability of hepta-vacancy

Case study 2 – Prismatic loops in Al

- Growth of planar vacancy clusters is predicted to be energetically favorable for sufficiently small concentrations
- Elucidation of relevant conditions requires large cell-size calculations
- Vacancy clustering and subsequent collapse is a possible mechanism for formation of prismatic dislocation loops
- Prismatic loops as small as those formed from hepta-vacancies are stable!

Concluding remarks

- Behavior of material samples may change radically with size (concentration): Small samples may not be representative of bulk behavior
- Need electronic structure calculations at macroscopic scales: Quasi-continuum OFDFT (QC/OFDFT)
- Outlook: Application to general materials requires extension to Kohn-Sham DFT…

Concluding remarks

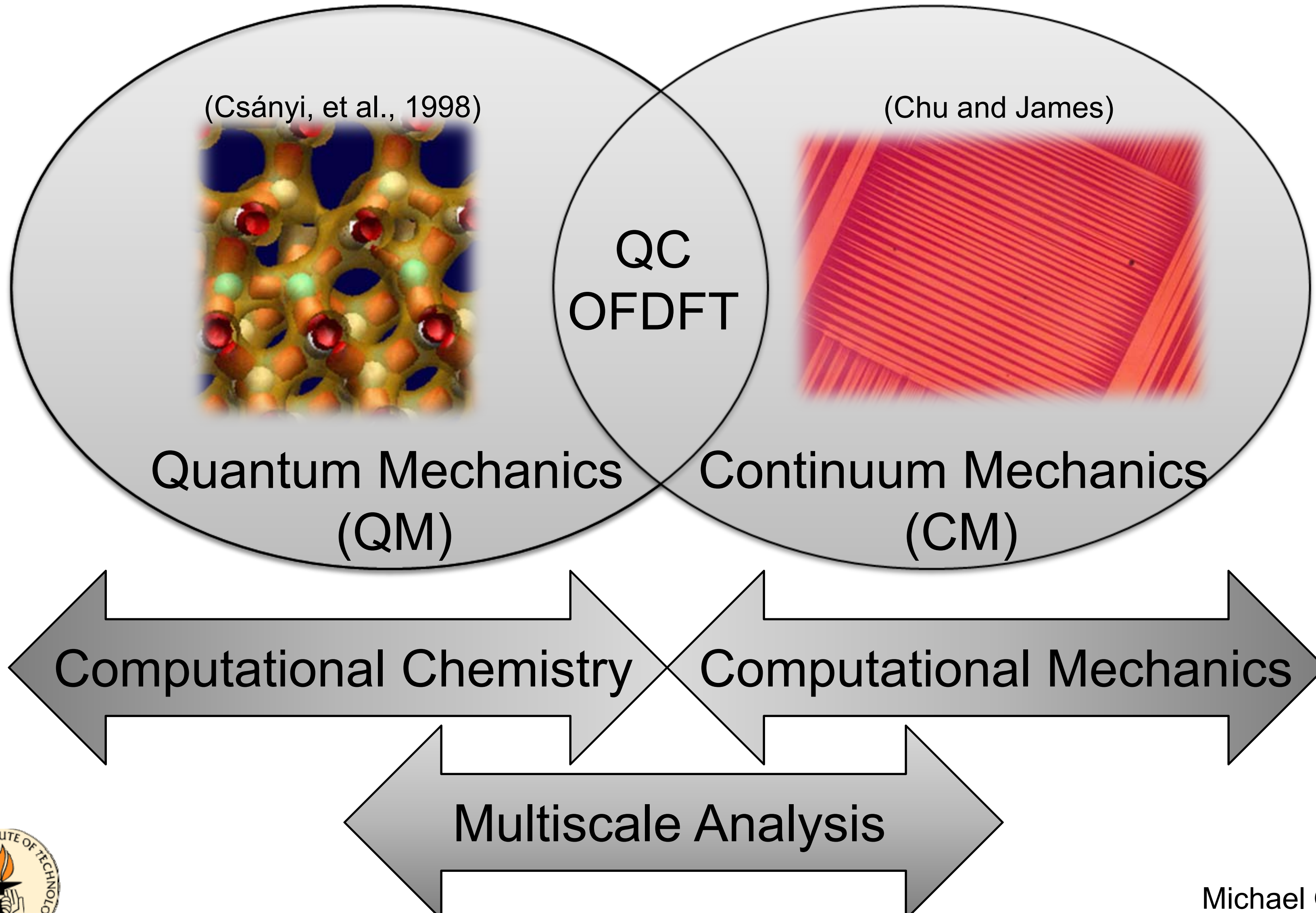

Concluding remarks

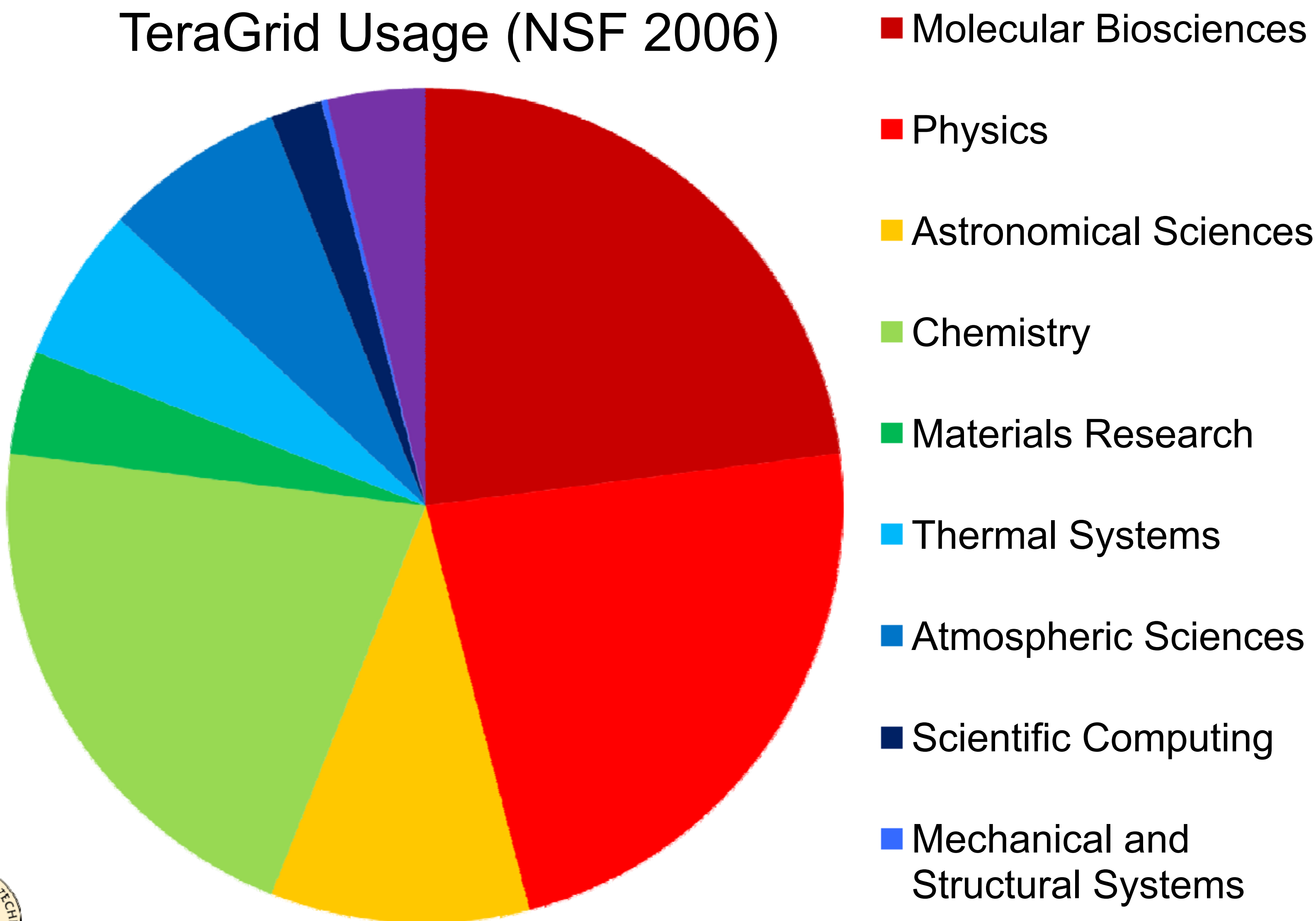

Concluding remarks

Institute for Mathematics and its Applications: Thematic Year on Mathematics and Chemistry

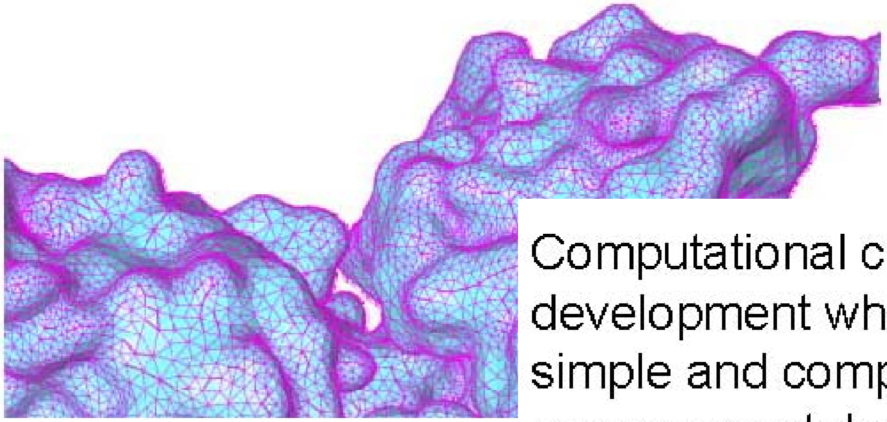

Computational chemistry has reached a stage of development where many chemical properties of both simple and complex systems may now be computed more accurately, more economically, or more speedily than they can be measured. Further advances in accuracy and practicality will depend on the development of both new theory and new algorithms. Mathematical techniques will play an important role in both of these areas.

Concluding remarks

Thank you!

Michael Ortiz
WCCM 07/01/08